

Renormalization-Group Flows and Fixed Points in Yukawa Theories

Esben Mølgaard^{a,b} and Robert Shrock^b

(a) *The Centre for Cosmology and Particle Physics Phenomenology CP³-Origins,
and the Danish Institute for Advanced Study DIAS,*

University of Southern Denmark, Campusvej 55, DK-5230 Odense M, Denmark and

(b) *C. N. Yang Institute for Theoretical Physics and Department of Physics and Astronomy
Stony Brook University, Stony Brook, NY 11794, USA*

We study renormalization-group flows in Yukawa theories with massless fermions, including determination of fixed points and curves that separate regions of different flow behavior. We assess the reliability of perturbative calculations for various values of Yukawa coupling y and quartic scalar coupling λ by comparing the properties of flows obtained with the beta functions of these couplings calculated to different orders in the loop expansion. The results provide a determination of the region in y and λ where calculations up to two loops can yield reasonably reliable results.

Preprint: CP³-Origins-2014-008 DNRf90, DIAS-2014-8; YITP-Stony Brook-2013-39

PACS numbers: 11.10.Hi, 11.15.Bt, 11.15.Pg

I. INTRODUCTION

The dependence of the coupling constants in a quantum field theory on the Euclidean momentum scale μ , at which they are measured is of fundamental importance. This behavior is described by the beta functions for these couplings [1]. In a theory with two or more couplings, a change in μ thus induces a renormalization-group (RG) flow in the space of couplings. The RG flow typically involves some infrared (IR) or ultraviolet (UV) fixed points, and one can characterize these as being attractive or repulsive along certain directions in the space of couplings. If the couplings are sufficiently small, then the respective beta functions can be reliably calculated perturbatively. As one or more of these couplings increases in magnitude, higher-loop contributions to the various beta functions become important, motivating calculations of these beta functions to higher loop order to obtain reliable results for RG flows (trajectories) and fixed points. If one or more couplings becomes too large, then it may not be possible to describe the RG flows, or, more generally, the properties of the theory, using perturbative calculations.

A general criterion for the reliability of a perturbative calculation is that if one calculates some quantity to a given loop order, then there should not be a large fractional change in this quantity if one computes it to one higher order in the loop expansion. Thus, in a situation where a putative fixed point occurs at moderately strong coupling, it is important to study how the value of the coupling(s) at this fixed point change(s) if one calculates the beta function(s) to higher loop order. For example, an asymptotically free non-Abelian gauge theory with sufficiently many fermions in a given representation has an IR fixed point (IRFP) [2]. If the number of fermions is only slightly less than the maximum allowed by the constraint of asymptotic freedom, this IRFP occurs at weak coupling [3]. As the number of fermions is decreased, the IRFP moves to stronger coupling, and

studies have been carried out of the effect of higher-loop terms in the beta function of the gauge coupling in this case [4]. One may also investigate a possible ultraviolet fixed point (UVFP) in an infrared-free theory such as U(1) gauge theory with higher-loop calculations (e.g., [5, 6] and references therein).

It is also of considerable interest to investigate renormalization-group flows in the more complicated case of quantum field theories that depend on more than one interaction coupling. There have been many studies of such flows for theories and ranges of momentum scale μ where the couplings are reasonably weak, so that perturbative calculations are reasonably accurate. This is the case for computations of RG flows of the SU(3)_c, SU(2)_L, and U(1)_Y gauge couplings in the Standard Model (SM) or the Minimal Supersymmetric Standard Model (MSSM) upward from a reference scale of, say, 1 TeV, up to higher scales such as 10^{16} GeV. There has also been interest in calculating the RG flow of the elements of Yukawa matrices in the SM and MSSM, and the quartic Higgs coupling λ_{SM} in the SM, from the 1 TeV scale to higher scales. Again, these RG flows can be reasonably well described by perturbative calculations, although with the measured value of the Higgs-like boson observed by the LHC, $m_H \simeq 126$ GeV (whence in the SM, $\lambda_{SM}(\mu) \simeq 0.13$ at $\mu = m_H$), in the absence of new physics effects at intermediate scales, it follows that $\lambda_{SM}(\mu)$ would decrease through zero at a high scale $\mu \sim 10^{10 \pm 1}$ GeV, implying that the SM, by itself, would be metastable above this scale [7]–[9].

In this paper we study renormalization-group flows in Yukawa theories and assess the reliability of perturbative calculations of these flows for a substantial range of Yukawa and quartic scalar couplings. The method that we use for this purpose is to compare the properties of flows that we obtain with the beta functions of these couplings calculated to different orders in the loop expansion. In order to focus on the essential features in as simple a framework as possible, we study scalar-fermion models

without any gauge fields. We construct these models so that the global symmetries forbid any Dirac or Majorana fermion mass terms, and we also consider the limit where scalar masses are negligibly small relative to the scales μ of interest. These models depend on two dimensionless couplings, a quartic self-coupling λ for the scalar field and a Yukawa coupling y . The beta functions for these couplings comprise a set of coupled first-order ordinary differential equations describing how the couplings vary as functions of μ . Integrating this set of differential equations, we determine their renormalization-group flows as functions of μ . To do this, we choose an initial scale, μ_0 , where the magnitudes of the couplings are sufficiently small that perturbative calculations may be reliable, and then perform the integration. Our method is to compare RG flows calculated using different loop orders for the two beta functions. We recall the basic fact that in these theories the quartic scalar self-coupling λ must be positive for the boundedness of the energy and equivalently the stability of the theory. As will be evident in our results, RG flows may take a theory with positive λ to one with negative λ . In this case, two comments are necessary. Strictly speaking, for a sufficiently small range of negative λ the theory may still be metastable, with a sufficiently long tunneling time that our perturbative calculations may be physically meaningful. However, for negative values of λ of sufficiently large magnitude, the theory is simply unstable, and the perturbative analysis is not applicable or meaningful. In most of our analytic discussions, therefore, we will implicitly take λ to be positive.

We remark on some earlier related work on Yukawa models. As is well known, Yukawa proposed such models [10] as an approach to understanding the binding of nucleons in nuclei, and pion exchange between nucleons does, indeed, play an important role in this binding. Of course, the physics here involves the exchange of a light approximate Nambu-Goldstone boson between two baryons, with the baryons being much heavier than the exchanged π meson, as indicated by the ratio of masses $m_\pi/m_N = 0.15$. This is quite different from our models, for which, by construction, a global chiral symmetry forbids any fermion mass fermions and the scalar mass is taken to be negligibly small relative to the interval of Euclidean momentum scales μ for which we integrate the beta functions to calculate the RG flows. Some early studies of perturbative RG equations for Standard Model Yukawa couplings included Refs. [11, 12]. It was recognized early on that the one-loop beta function for a scalar theory without fermions is positive, this theory is, perturbatively, at least, IR-free; that is, as $\mu \rightarrow 0$, $\lambda(\mu) \rightarrow 0$. However, it was also recognized that if one adds fermions to this scalar theory to get a full scalar-fermion Yukawa theory, then the fermions contribute a negative term proportional to y^4 in the beta function $d\lambda/d\ln\mu$, and hence, for sufficiently large y , this can reverse the sign of the full one-loop term in this beta function and hence possibly render the scalar coupling in

the Yukawa theory nontrivial [12]. This motivated fully nonperturbative studies, and these were carried out using lattice studies with dynamical fermions [13] (some recent work includes [14]). One may obtain a Yukawa theory starting from a full gauge-fermion-Higgs theory by turning off the gauge couplings. In this framework, a natural approach is to start with a chiral gauge theory (exemplified by the Standard Model), which forbids bare fermion masses in the Lagrangian. However, owing to fermion doubling on the lattice, it has been challenging to implement chiral gauge theories on the lattice. We believe, therefore, that there is continuing interest in pursuing analyses of renormalization-group evolution of continuum Yukawa theories using perturbatively calculated beta functions. Indeed, simple scalar-fermion models have been of recent interest in studies of quasi-scale invariant behavior (e.g., [15]; see also [9, 16]).

This paper is organized as follows. In Sect. II we define our notation for the relevant variables and beta functions. In Sect. III we study a scalar-fermion model with an $SU(2) \otimes U(1)$ global symmetry group. In Sect. IV we generalize this analysis to a model with N_f copies (“flavors”) of fermions and an $SU(N) \otimes SU(N_f) \otimes U(1)$ global symmetry group. Our conclusions are contained in Sect. V.

II. BETA FUNCTIONS

The beta functions describing the dependence of the running couplings $y = y(\mu)$ and $\lambda = \lambda(\mu)$ on the scale μ where they are measured are

$$\beta_y \equiv \frac{dy}{dt}, \quad \beta_\lambda \equiv \frac{d\lambda}{dt}, \quad (2.1)$$

where $dt = d\ln(\mu/\mu_0)$, where μ_0 is an initial value of the reference scale. (The μ dependence of y and λ is implicitly understood below but the argument will often be suppressed in the notation.) These beta functions can be expressed as a sum of ℓ -loop terms as

$$\beta_y = \sum_{\ell=1}^{\infty} \frac{b_y^{(\ell)}}{(4\pi)^{2\ell}}, \quad \beta_\lambda = \sum_{\ell=1}^{\infty} \frac{b_\lambda^{(\ell)}}{(4\pi)^{2\ell}}, \quad (2.2)$$

where $b_y^{(\ell)}/(4\pi)^{2\ell}$ and where $b_\lambda^{(\ell)}/(4\pi)^{2\ell}$ denote the ℓ -loop contributions to β_y and β_λ , respectively.

It will also be convenient to define the variables

$$a_y \equiv \frac{y^2}{(4\pi)^2}, \quad a_\lambda \equiv \frac{\lambda}{(4\pi)^2}, \quad (2.3)$$

which will be used for the $SU(2) \otimes U(1)$ model studied below. For the $SU(N) \otimes SU(N_f) \otimes U(1)$ model and, in particular, for the limit (4.4), we define the variables

$$\bar{a}_y \equiv \frac{y^2 N}{(4\pi)^2}, \quad \bar{a}_\lambda \equiv \frac{\lambda N}{(4\pi)^2}. \quad (2.4)$$

Correspondingly, for the $SU(2) \otimes U(1)$ model we define the beta functions

$$\beta_{a_y} \equiv \frac{da_y}{dt} = \frac{2y}{(4\pi)^2} \beta_y, \quad \beta_{a_\lambda} \equiv \frac{da_\lambda}{dt} = \frac{1}{(4\pi)^2} \beta_{a_\lambda}, \quad (2.5)$$

with the series expansions

$$\beta_{a_y} = \sum_{\ell=1}^{\infty} b_{a_y}^{(\ell)}, \quad \beta_{a_\lambda} = \sum_{\ell=1}^{\infty} b_{a_\lambda}^{(\ell)}. \quad (2.6)$$

From the relations above, it follows that

$$b_{a_y}^{(\ell)} = \frac{2y}{(4\pi)^{2(\ell+1)}} b_y^{(\ell)}, \quad b_{a_\lambda}^{(\ell)} = \frac{1}{(4\pi)^{2(\ell+1)}} b_\lambda^{(\ell)} \quad (2.7)$$

We denote the n -loop ($n\ell$) beta functions as $\beta_{a_y, n\ell}$ and $\beta_{a_\lambda, n\ell}$.

Similarly, for the $SU(N) \otimes SU(N_f) \otimes U(1)$ model, we define the beta functions

$$\beta_{\bar{a}_y} \equiv \frac{d\bar{a}_y}{dt} = \frac{2yN}{(4\pi)^2} \beta_y \quad (2.8)$$

and

$$\beta_{\bar{a}_\lambda} \equiv \frac{d\bar{a}_\lambda}{dt} = \frac{N}{(4\pi)^2} \beta_\lambda \quad (2.9)$$

with series expansions analogous to those in Eq. (2.6) with a_y and a_λ replaced by \bar{a}_y and \bar{a}_λ , respectively. In the latter case, the LNN limit (4.4) will generally be understood.

As discussed in the introduction, these beta functions form a set of two coupled differential equations. We integrate these for each of the two models that we study to calculate the resultant RG flows. A point in the multidimensional space of couplings where all of the beta functions vanish simultaneously is, formally, a renormalization-group fixed point (FP). In general, RG flows may include the presence of one or more ultraviolet (UV) fixed point(s) if the beta functions vanish as $\mu \rightarrow \infty$ and/or infrared (IR) fixed point(s), where the beta functions vanish as $\mu \rightarrow 0$. In general, a fixed point may be stable along some directions and unstable along others. If the particle content of the theory does not change along the RG flow from μ_0 to the fixed point, then it is an exact UV or IR fixed point. In the vicinity of a (formal) fixed point, the RG flows are slow, so that the theories exhibit approximate scale-invariance.

For our comparative study we will perform the integrations to calculate the RG flows with the beta functions β_{a_y} and β_{a_λ} calculated to various different loop orders. We denote these as follows. For the $SU(2) \otimes U(1)$ model, the calculation using the $\beta_{a_y, n\ell}$ and $\beta_{a_\lambda, k\ell}$ beta functions is denoted (n, k) . The specific cases for which we perform the integrations are

- (1,1), i.e., $\beta_{a_y, 1\ell}$ and $\beta_{a_\lambda, 1\ell}$
- (1,2), i.e., $\beta_{a_y, 1\ell}$ and $\beta_{a_\lambda, 2\ell}$

- (2,1), i.e., $\beta_{a_y, 2\ell}$ and $\beta_{a_\lambda, 1\ell}$
- (2,2), i.e., $\beta_{a_y, 2\ell}$ and $\beta_{a_\lambda, 2\ell}$

We use the same notation to describe the four cases for the $SU(N) \otimes SU(N_f) \otimes U(1)$ model, so that in this context, the case (1,1) refers to an RG calculation using $\beta_{\bar{a}_y, 1\ell}$ and $\beta_{\bar{a}_\lambda, 1\ell}$ and so forth for the other cases. Some remarks are in order here. For a perturbative calculation of quantities in a theory with multiple couplings, a general procedure would be to calculate to similar orders in the various couplings if they are equally large and significant for the physics, and to calculate to higher order in a coupling that is larger. Thus, for example, in a Standard-Model process, one may only need to calculate to lowest order in electroweak couplings, but to higher order in the QCD coupling. Such a calculation is consistent in the sense that one has included higher-order terms in a larger coupling. Ref. [9] obtained the result that Weyl consistency conditions are maintained only if one uses the beta functions $\beta_{a_g, (n+2)\ell}$, $\beta_{a_y, (n+1)\ell}$, and $\beta_{a_\lambda, n\ell}$, where g denotes a gauge coupling and $a_g \equiv g^2/(4\pi)^2 = \alpha/(4\pi)$ (see also [17]).

In this type of study there are several obvious caveats. First, clearly, as couplings increase in strength, perturbative calculations become progressively less reliable. This is, indeed, a motivation for our present work - to assess quantitatively where this reduction in reliability occurs in the case of scalar-fermion models depending on two coupling constants. Second, higher-loop terms in beta functions of multi-coupling theories are generically scheme-dependent, and the positions of fixed points are hence also scheme-dependent. Indeed, scheme dependence is also present in higher-loop calculations in quantum chromodynamics (QCD). As in common practice in QCD, we use results computed with the \overline{MS} scheme [18]. One can assess the effect of scheme dependence of RG flows and fixed points by comparing these in different schemes [4]. However, many scheme transformations that are acceptable in the vicinity of a fixed point at zero coupling (e.g., a UVFP in an asymptotically free gauge theory, or an IRFP in an infrared-free theory) are not acceptable at a fixed point that occurs at a moderately strong coupling, because they produce various unphysical pathologies [6, 19, 20]. A third caveat, related to the first, is that if one or more of the couplings is (are) sufficiently large, the Yukawa and/or quartic scalar self-interaction may lead to nonperturbative phenomena such the formation of a fermion condensate, a vacuum expectation value (VEV) for the scalar field, and/or fermion-fermion bound states (see, e.g., [16], [21]). In the case where the coefficient of the quadratic term in the scalar potential V is zero, there is the related possibility of a nonperturbative generation of a nonpolynomial term in V , whose minimum could lead to a nonzero VEV for the scalar field [22]. Early studies of the stability of a theory in the presence of this phenomenon and associated related bounds on fermion and Higgs masses include [12, 23].

If fermion condensation occurs at some scale μ_c (where

the subscript c for condensate) in the vicinity of a formal IR fixed point, then the originally massless fermions gain dynamical masses, spontaneously breaking the approximate scale invariance in the theory near to an apparent RG fixed point. In the low-energy effective field theory applicable for scales $\mu < \mu_c$, one integrates these fermions out, thereby obtaining different beta functions. Thus, in this case, the formal fixed point would only be approximate rather than exact, since after the fermion condensation, the beta functions and flows would be different. This spontaneous symmetry breaking (SSB) of the approximate scale invariance generically leads to the appearance of a corresponding Nambu-Goldstone boson, the dilaton. This dilaton is not massless, since the beta functions in the vicinity of the fixed point were small but not precisely zero.

If $\mu_\phi^2 < 0$ so that there is a VEV for the scalar field, then the Yukawa coupling leads to a mass for the fermion field(s) of the form $m_f \propto yv$. However, since the VEV $v = (-\mu_\phi^2/\lambda)^{1/2}$ and since we assume that $|\mu_\phi|$ is much smaller than the reference scales μ over which we integrate the renormalization-group equations, it follows that for moderate values of the ratio y^2/λ , the resultant fermion masses $m_f \propto y(-\mu_\phi^2/\lambda)^{1/2}$ are negligible relative to the interval of μ that we study.

III. $SU(2) \otimes U(1)$ MODEL

A. Field Content and Symmetry Group

The first model that we study is motivated by the leptonic sector of the Standard Model, with the gauge interactions turned off. It includes a fermion ψ_L^a which is a doublet under $SU(2)$ with weak hypercharge Y_ψ and a χ_R , which is a singlet under $SU(2)$ with weak hypercharge Y_χ , together with the usual scalar field ϕ^a transforming as a doublet under $SU(2)$ with weak hypercharge Y_ϕ . Here, $a = 1, 2$ is an $SU(2)$ group index which will often be suppressed in the notation. We assume that these hypercharges are nonzero and that $Y_\psi \neq Y_\chi$. Since we have set the gauge couplings to zero, the $SU(2) \otimes U(1)$ is a global symmetry group. As in the Standard Model, we set

$$Y_\phi = Y_\psi - Y_\chi \quad (3.1)$$

to ensure that the Yukawa interaction term is invariant under the global symmetry. The Lagrangian for this model is

$$\begin{aligned} \mathcal{L} = & \bar{\psi}_L i \not{\partial} \psi_L + \bar{\chi}_R i \not{\partial} \chi_R - [y \bar{\psi}_L \chi_R \phi + h.c.] \\ & + \partial_\mu \phi^\dagger \partial^\mu \phi - \mu_\phi^2 \phi^\dagger \phi - \lambda (\phi^\dagger \phi)^2. \end{aligned} \quad (3.2)$$

Without loss of generality, we can make $y(\mu_0)$ real and positive at a given value μ_0 (by changing the phase of ψ_L or χ_R or ϕ). We assume that this is done. We allow μ_ϕ^2 of either sign but assume that $|\mu_\phi^2|$ is negligibly small

compared with the range of μ^2 of interest for our study of RG flows [24] (see also the end of Section II). The global $SU(2)$ symmetry forbids the Majorana bilinear $\psi_L^a, {}^T C \psi_L^b$ and the Dirac bilinear $\bar{\psi}_{a,L} \chi_R$ from occurring in \mathcal{L} . Since Y_χ is taken to be nonzero, the $U(1)$ symmetry forbids the Majorana bilinear $\chi_R^T C \chi_R$ (as well as $\psi_L^a, {}^T C \psi_L^b$ and $\bar{\psi}_{a,L} \chi_R$ bilinears). Thus, the condition that \mathcal{L} be invariant under this global symmetry group implies that the fermions are massless.

B. Beta Functions

The one-loop and two-loop coefficients in the beta functions β_y and β_λ can be extracted, with the requisite changes to match our normalizations, from previous calculations (which were done in the \overline{MS} scheme) [8, 11, 25]. They are

$$b_y^{(1)} = \frac{5}{2} y^3 \quad (3.3)$$

$$b_y^{(2)} = 3y(-y^4 - 4y^2\lambda + 2\lambda^2) \quad (3.4)$$

$$b_\lambda^{(1)} = 2(12\lambda^2 + 2y^2\lambda - y^4) \quad (3.5)$$

$$b_\lambda^{(2)} = -312\lambda^3 - 48y^2\lambda^2 - y^4\lambda + 10y^6. \quad (3.6)$$

In terms of the variables a_y and a_λ used for the figures,

$$b_{a_y}^{(1)} = 5a_y^2 \quad (3.7)$$

$$b_{a_y}^{(2)} = 6a_y(-a_y^2 - 4a_y a_\lambda + 2a_\lambda^2) \quad (3.8)$$

$$b_{a_\lambda}^{(1)} = 2(12a_\lambda^2 + 2a_y a_\lambda - a_y^2) \quad (3.9)$$

$$b_{a_\lambda}^{(2)} = -312a_\lambda^3 - 48a_y a_\lambda^2 - a_y^2 a_\lambda + 10a_y^3. \quad (3.10)$$

We comment on some properties of β_y or equivalently, β_{a_y} . We recall that at the initial point μ_0 where we start our integrations of the renormalization group equations, we have, with no loss of generality, rendered y real and positive. A first comment is that because β_y has an overall factor of y , and β_{a_y} has an overall factor of a_y , it follows that the flow in y can never take y through zero to negative values of y , and the flow in a_y can never take a_y through zero to negative values of a_y .

The fact that $b_{a_y}^{(1)} > 0$ means that for sufficiently small a_y and a_λ , $\beta_{a_y} > 0$, i.e., as μ decreases from the UV to the IR, the Yukawa coupling y decreases. At the two-loop level,

$$b_{a_y}^{(2)} > 0 \quad \text{if} \quad a_\lambda > (1 + \sqrt{3/2}) a_y = 2.2247 a_y, \quad (3.11)$$

to the given floating-point accuracy. If these conditions are satisfied, then the two-loop coefficient contributes to β_{a_y} with the same sign as the one-loop coefficient and increases the rate of change of a_y as a function of μ . If, on the other hand $a_\lambda < (1 + \sqrt{3/2})a_y$, then $b_{a_y}^{(2)} < 0$, so $b_{a_y}^{(2)}$ contributes to β_{a_y} with a sign opposite to that of $b_{a_y}^{(1)}$. In this case, it is possible for β_{a_y} to vanish at the two-loop level. The condition for this to happen is that either $a_y = 0$ for some μ or (again suppressing the argument, μ) that

$$5a_y + 6(-a_y^2 - 4a_y a_\lambda + 2a_\lambda^2) = 0. \quad (3.12)$$

Solving this equation for a_y yields the physical solution

$$a_y = \frac{5}{12} - 2a_\lambda + \frac{1}{12}\sqrt{864a_\lambda^2 - 240a_\lambda + 25}. \quad (3.13)$$

(The polynomial in the square root is positive-definite.) Equivalently, solving Eq. (3.12) for a_λ yields

$$a_\lambda = a_y + \frac{1}{6}\sqrt{3a_y(18a_y - 5)}, \quad (3.14)$$

which is physical if $a_y \geq 5/18$, i.e., $y \geq (4\pi/3)\sqrt{5/2} = 6.623$. Evidently, this zero of $\beta_{a_y, 2\ell}$ is only possible for such large values of y that one must anticipate significant corrections from higher-loop terms in β_{a_y} . In passing, we note that the other solution of Eq. (3.12) for λ with a minus sign in front of the square root is unphysical, since it can lead to a negative λ . (As noted before, we do not attempt to consider a metastable situation with a negative λ of small magnitude.) Also, the other solution of Eq. (3.12) for a_y with a minus sign in front of the square root in Eq. (3.13) is unphysical because it can lead to a value of $a_y < 5/18$. Setting $a_y = 5/18$ in Eq. (3.14) yields $a_\lambda = a_y = 5/18$, and similarly, setting $a_\lambda = 5/18$ in Eq. (3.13) yields $a_y = a_\lambda = 5/18$.

We next remark on some properties of β_{a_λ} . We find that

$$b_{a_\lambda}^{(1)} = 0 \quad \text{if} \quad a_\lambda = \frac{(\sqrt{13} - 1)}{12} a_y = 0.21713 a_y \quad (3.15)$$

and

$$b_{a_\lambda}^{(1)} > 0 \quad \text{if} \quad a_\lambda > \frac{(\sqrt{13} - 1)}{12} a_y, \quad (3.16)$$

or equivalently, $a_y < (1 + \sqrt{13})a_\lambda = 4.60555a_\lambda$. The condition that $b_{a_\lambda}^{(2)} = 0$ is a cubic equation in a_λ and separately a cubic equation in a_y . We find that if $a_y = (1 + \sqrt{13})a_\lambda$, so that $b_{a_\lambda}^{(1)} = 0$, then

$$b_{a_\lambda}^{(2)} = \frac{2(13 + 55\sqrt{13})}{(4\pi)^6} \lambda^3 = (1.073 \times 10^{-4}) \lambda^3. \quad (3.17)$$

Hence, if the values of a_λ and $a_y \neq 0$ are such that the one-loop contribution to $\beta_{a_\lambda} = 0$, then at the two-loop level, $\beta_{a_\lambda} > 0$.

In the special case where $a_y = 0$, we find that if we consider $\beta_{a_\lambda, 2\ell}$, a non-trivial fixed point appears at

$$a_\lambda^* = \frac{1}{13} = 0.076923. \quad (3.18)$$

This fixed point is repulsive in the a_y -direction, since for lower values of a_λ (while keeping $a_y = 0$), $b_{a_\lambda}^{(1)}$ drives the flow down, and for higher, $b_{a_\lambda}^{(2)}$ drives it up.

We next give some illustrative numerical evaluations. Let us consider that the theory is such that at some reference scale μ_0 , $y(\mu_0)$ and $\lambda(\mu_0)$ have the values $y(\mu_0) = 1$ and $\lambda(\mu_0) = 1$. If one were to consider turning on gauge fields (and adding quarks so that this theory is free of gauge anomalies), then these would be rather large physical values of these couplings. For reference, considering only the third generation in the Standard Model (SM) and using the relation for a fermion mass in terms of the Yukawa coupling and the Higgs vacuum expectation value, $\langle\phi\rangle_0$, namely

$$y_f \langle\phi\rangle_0 = y_f \frac{v}{\sqrt{2}} = m_f, \quad (3.19)$$

where $v = 246$ GeV, one has the rough values $y_\tau \simeq 1 \times 10^{-2}$, $y_b \simeq 2 \times 10^{-2}$, and $y_t \simeq 1$. Further, using the relation for the Higgs boson mass m_H in the Standard Model, namely,

$$m_H = (2\lambda)^{1/2} v \quad (3.20)$$

one has $\lambda(\mu) = 0.13$ at $\mu = m_H = 126$ GeV, as noted above. So the illustrative reference values $y(\mu_0) = \lambda(\mu_0) = 1$ that we have taken may be considered to be reasonably large. Nevertheless, the variables that enter in the beta functions are then rather small because they involve a factor of $1/(4\pi^2)$; $a_y(\mu) = \lambda(\mu) = 1/(4\pi)^2 = 0.6333 \times 10^{-2}$. In the beta function β_{a_y} , the one-loop term $b_{a_y}^{(1)} = 2.005 \times 10^{-4}$, and the two-loop term $b_{a_y}^{(2)} = -0.4571 \times 10^{-5}$, so that the ratio of the two-loop to one-loop terms is

$$y = \lambda = 1 \Rightarrow \frac{b_{a_y}^{(2)}}{b_{a_y}^{(1)}} = -0.02280. \quad (3.21)$$

In the beta function β_{a_λ} , the one-loop term $b_{a_\lambda}^{(1)} = 1.043 \times 10^{-3}$ and $b_{a_\lambda}^{(2)} = -0.89135 \times 10^{-4}$, so that

$$y = \lambda = 1 \Rightarrow \frac{b_{a_\lambda}^{(2)}}{b_{a_\lambda}^{(1)}} = -0.0855. \quad (3.22)$$

We also note the values of the one-loop and two-loop beta functions for a_y and a_λ :

$$y = \lambda = 1 \Rightarrow \frac{\beta_{a_y, 1\ell}}{\beta_{a_\lambda, 1\ell}} = \frac{b_{a_y}^{(1)}}{b_{a_\lambda}^{(1)}} = 0.1923 \quad (3.23)$$

and

$$y = \lambda = 1 \Rightarrow \frac{\beta_{a_y, 2\ell}}{\beta_{a_\lambda, 2\ell}} = \frac{b_{a_y}^{(1)} + b_{a_y}^{(2)}}{b_{a_\lambda}^{(1)} + b_{a_\lambda}^{(2)}} = 0.2055 \quad (3.24)$$

Thus, for this illustrative case with $y(\mu_0) = \lambda(\mu_0) = 1$, the two-loop term in β_{a_y} makes only a small contribution relative to the one-loop term, so that the perturbative expansion for β_{a_y} is reasonably reliable to this two-loop order, and similarly for β_{a_λ} .

C. RG Flows

To study the RG flows in this model, we begin by finding the fixed points, that is the solutions to the simultaneous conditions $\beta_{a_y, n\ell} = 0$, $\beta_{a_\lambda, k\ell} = 0$ for the values of loop orders (n, k) that we consider. We first note that the IR-free (trivial) fixed point

$$a_y^* = 0, \quad a_\lambda^* = 0, \quad (3.25)$$

is a solution to the beta functions for any of our (n, k) cases. Beyond this IR-free fixed point, we find that the choice of loop order (n, k) in the beta functions is quite important for the appearance and location of fixed points. From Eqs. (3.7)-(3.10), we calculate the fixed point to be as follows:

$$\text{case } (1, 1) \Rightarrow \text{no nonzero fixed points.} \quad (3.26)$$

$$\text{case } (1, 2) \Rightarrow a_y^* = 0, \quad a_\lambda^* = \frac{1}{13} = 0.07692. \quad (3.27)$$

$$\begin{aligned} \text{case } (2, 1) \Rightarrow a_y^* &= \frac{5}{318}(13\sqrt{13} - 17) = 0.4697, \\ a_\lambda^* &= \frac{5}{638}(31 - 5\sqrt{13}) = 0.1020. \end{aligned} \quad (3.28)$$

$$\text{case } (2, 2) \Rightarrow \text{two fixed points :}$$

$$\begin{aligned} a_y^* &= 0, \quad a_\lambda^* = \frac{1}{13} = 0.07692 \text{ and} \\ a_y^* &= 0.4104, \quad a_\lambda^* = 0.1247. \end{aligned} \quad (3.29)$$

The presence of a fixed point for such a low value of a_λ as $1/13$ means that only a very small region of coupling space is independent of the choice of (n, k) . In Fig. 1, we see that the flows change character based on (n, k) when both a_y and a_λ are larger than approximately 0.04. Note, in particular, that the plots where the two-loop term $b_{a_\lambda}^{(2)}$ is included in β_{a_λ} have concave flows towards the trivial fixed point, whereas the ones where it is not have convex flows towards the same in this region.

If we let a_y and a_λ increase beyond $1/(4\pi)$, changes appear quite rapidly (see Fig. 2), which means that one cannot trust the perturbative analysis to these orders in this region of couplings. With this caveat in mind, we shall proceed to describe the RG flows. The first striking difference is that if the two-loop term $\beta_{a_\lambda}^{(2)}$ in the

beta function β_{a_λ} is included, then the flow ending in the partially attractive fixed point at $a_y^* = 0, a_\lambda^* = 1/13$ is a separatrix which divides a region where the flows end in the trivial fixed point at the origin, from one where they increase to large values of a_λ . The plots in this and the other figures were generated using the Mathematica StreamPlot routine. (Because the integration routine can lose some numerical accuracy when the beta functions approach zero near fixed points, it does not show arrows and associated RG flows very close to these fixed points.)

The second is that including the two-loop term in the Yukawa beta function produces a fixed point where neither of the couplings is zero. However, the impact that this has on the flow is very different in the (2,1) and (2,2) cases. In the (2,1) case, the fixed point is partially attractive, and the flow that reaches it from above forms a separatrix, separating a region where the flows end at the origin from a region where they move toward larger values of a_y in the IR. In the (2,2) case, the fixed point is totally repulsive, and the dominant term in the beta functions is the a_λ^3 term in equation (3.10). This term drives every flow, above the one originating in the eigendirection of positive a_y from the fixed point (marked in red on Fig. 2), towards larger a_λ in the IR, which in turn means that the dominant term in $\beta_{a_y, 2\ell}$ will eventually be the $a_y a_\lambda^2$ term, which drives $a_y \rightarrow 0$ in the IR.

For the (2,2) flows that originate at the totally repulsive fixed point and go in the direction of negative a_λ , there is a delicate balance between terms driving them towards the origin and terms driving them towards highly negative a_λ in the IR. This balance is manifested in the stable manifold (marked in green on Fig. 2) which separates the regions of convergence to the origin and flow to (unphysical) negative values.

IV. $SU(N) \otimes SU(N_f) \otimes U(1)$ MODEL

A. Field Content, Symmetry Group, and LNN Limit

In this section we study a model that is a two-fold generalization of the model in the previous section. First, we construct the model so that it is invariant under a global symmetry group

$$G = SU(N) \otimes SU(N_f) \otimes U(1), \quad (4.1)$$

rather than the $SU(2) \otimes U(1)$ group of the previous model. We include an N_f -fold replication of the left-handed and right-handed fermions. The fermion content consists of (i) $\psi_{j,L}^a$, transforming as a (\square, \square) representation of $SU(N) \otimes SU(N_f)$, where a is an $SU(N)$ group index taking on the values $a = 1, \dots, N$, and j is a copy ("flavor") index, taking on the values $j = 1, \dots, N_f$; and (ii) $\chi_{j,R}$, with $j = 1, \dots, N_f$, transforming as a $(1, \square)$ representation of $SU(N) \otimes SU(N_f)$. The model also has a scalar field ϕ^a transforming as a $(\square, 1)$ representation of

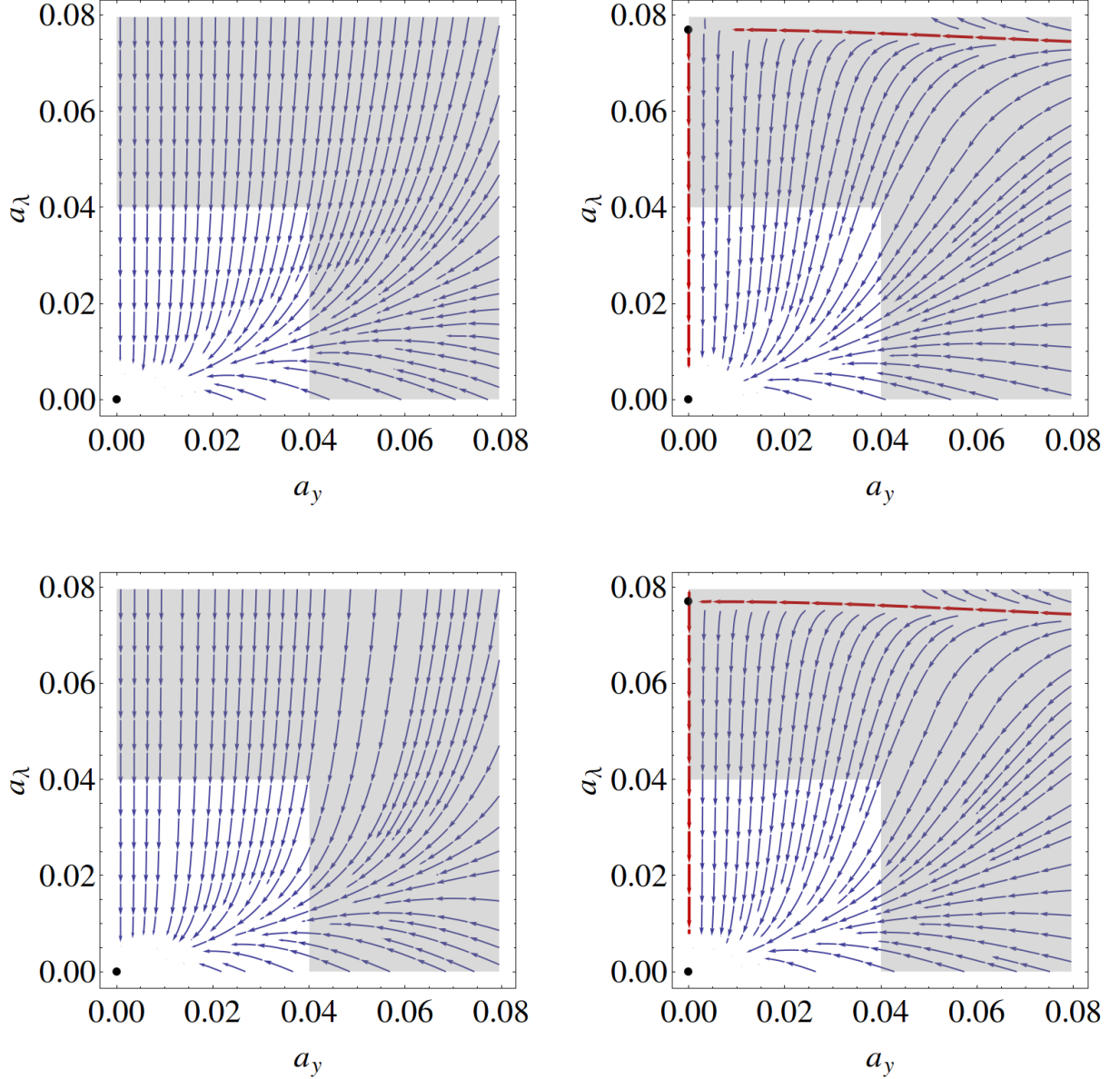


FIG. 1: The renormalization-group flows for the $SU(2) \otimes U(1)$ model with $0 \leq a_y \leq 1/(4\pi)$ and $0 \leq a_\lambda \leq 1/(4\pi)$. The white square region is where $0 \leq a_y \leq 0.04$ and $0 \leq a_\lambda \leq 0.04$, and the gray region occupies the rest of the plot. The figures correspond to the following different choices of loop order in the beta functions: (1,1) (upper left); (1,2) (upper right); (2,1) (lower left); and (2,2) (lower right). The red flows for the cases (1,2) and (2,2) originate along the eigendirections of the fixed points.

$SU(N) \otimes SU(N_f)$. The hypercharges are again taken to be nonzero and to satisfy the conditions that $Y_\psi \neq Y_\chi$ and Eq. (3.1). The transformations of $\psi_{j,L}^a$ and $\chi_{j,R}$ under $SU(N_f)$ are

$$\psi_{j,L}^a \rightarrow \sum_{k=1}^{N_f} U_{jk} \psi_{k,L}^a, \quad \chi_{j,R} \rightarrow \sum_{k=1}^{N_f} U_{jk} \chi_{k,R} \quad (4.2)$$

where $U \in SU(N_f)$.

The Lagrangian of this model is

$$\begin{aligned} \mathcal{L} = & \sum_{j=1}^{N_f} \left[\bar{\psi}_{j,L} i \not{\partial} \psi_{j,L} + \bar{\chi}_{j,R} i \not{\partial} \chi_{j,R} \right] \\ & - y \sum_{j=1}^{N_f} [\bar{\psi}_{j,L} \chi_{j,R} \phi + h.c.] \\ & + \partial_\mu \phi^\dagger \partial^\mu \phi - \mu_\phi^2 \phi^\dagger \phi - \lambda (\phi^\dagger \phi)^2, \end{aligned} \quad (4.3)$$

where we have suppressed $SU(N)$ indices in the nota-

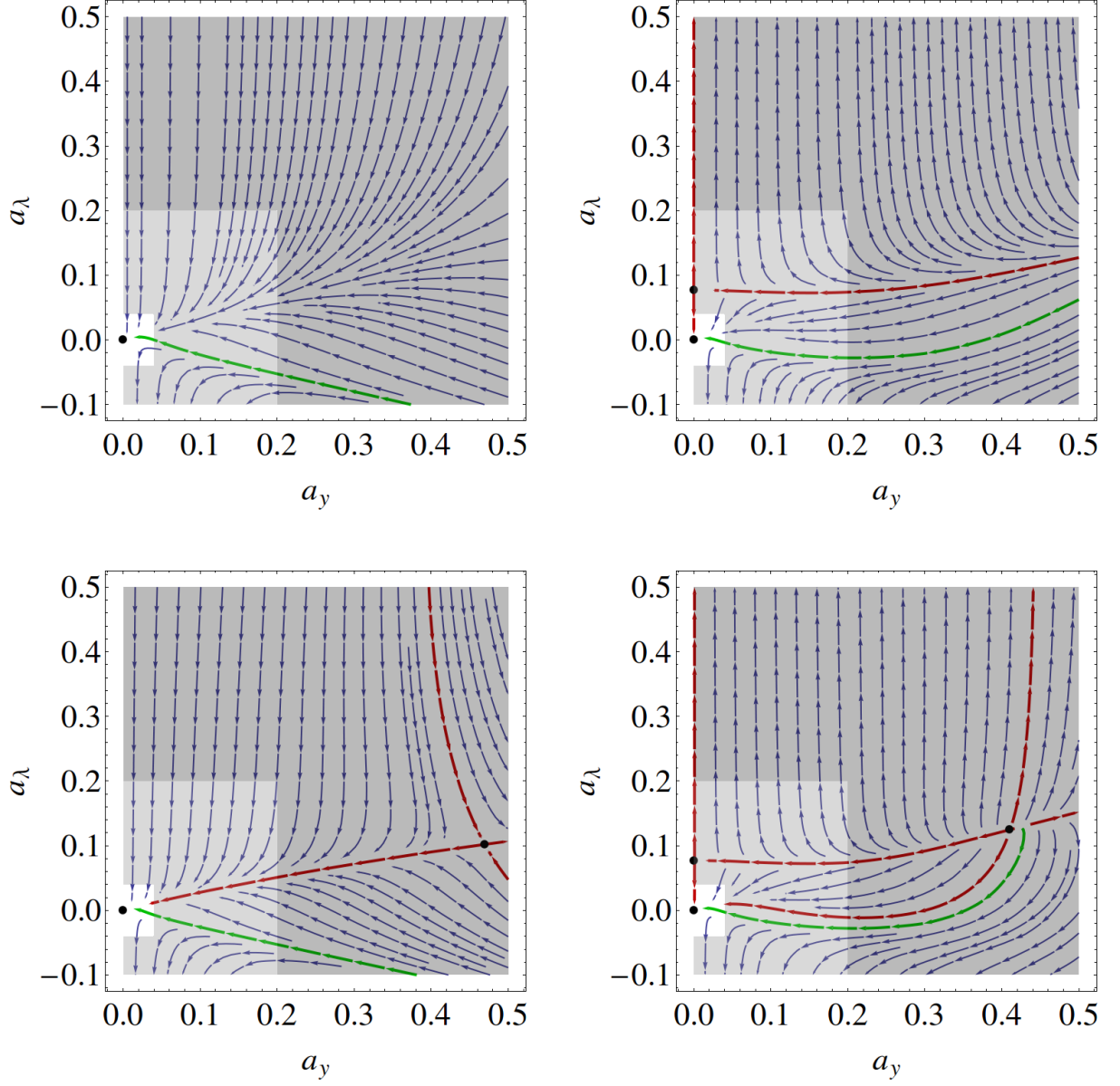


FIG. 2: The renormalization-group flows for the $SU(2) \otimes U(1)$ model with $0 \leq a_y \leq 0.5$ and $-0.1 \leq a_\lambda \leq 0.5$. The white region is where $0 \leq a_y \leq 0.04$ and $-0.1 \leq a_\lambda \leq 0.04$; the light gray region is where $0.04 \leq a_y \leq 0.2$ and $-0.1 \leq a_\lambda \leq 0.2$; and the dark gray region occupies the rest of the figure. The figures correspond to the following different choices of loop order in the beta functions: (1,1) (upper left); (1,2) (upper right); (2,1) (lower left); and (2,2) (lower right). The green flows are the stable manifolds in coupling constant space which bound the basins of attraction of the fixed point at the origin. The red flows in (1,2), (2,1) and (2,2) originate along the eigendirections of the fixed points.

tion. The $SU(N) \otimes U(1)$ symmetry forbids the fermion bilinears $\psi_{j,L}^a C \psi_{k,L}^b$, $\chi_{j,R}^T C \chi_{k,R}$, and $\bar{\psi}_{a,j,L} \chi_{k,R}$, so the fermions are massless. Our requirement of $SU(N_f)$ invariance restricts the Yukawa coupling to the form given in Eq. (4.3). As before, we allow either sign of μ_ϕ^2 and impose the condition that $|\mu_\phi|$ be negligibly small relative to the range of μ over which we calculate the RG flows (see also the end of Section II).

One of the motivations for this generalization is that

it enables us to take the combined limit

$$\begin{aligned}
 N &\rightarrow \infty, \quad N_f \rightarrow \infty \quad \text{with } r \equiv \frac{N_f}{N} \text{ fixed} \\
 y &\rightarrow 0, \quad \lambda \rightarrow 0 \quad \text{with } \bar{a}_y \text{ and } \bar{a}_\lambda \text{ being} \\
 &\text{finite functions of } \mu
 \end{aligned} \tag{4.4}$$

We will use the symbol \lim_{LNN} for this limit, where “LNN” stands for “large N_c and N_f ”

B. Beta Functions

To simplify the analysis, we take the LNN limit (4.4). In this limit, from [25] (see also [8]) we find

$$b_{\bar{a}_y}^{(1)} = (1 + 2r)\bar{a}_y^2 \quad (4.5)$$

$$b_{\bar{a}_y}^{(2)} = -3r\bar{a}_y^3 \quad (4.6)$$

$$b_{\bar{a}_\lambda}^{(1)} = 2(2\bar{a}_\lambda^2 + 2r\bar{a}_y\bar{a}_\lambda - r\bar{a}_y^2) \quad (4.7)$$

and

$$b_{\bar{a}_\lambda}^{(2)} = r\bar{a}_y(-8\bar{a}_\lambda^2 - 3\bar{a}_y\bar{a}_\lambda + 2\bar{a}_y^2). \quad (4.8)$$

We remark on some general properties of these terms. First, because $\beta_{\bar{a}_y}$ has an overall factor of \bar{a}_y , it follows that the flow in \bar{a}_y can never take \bar{a}_y through zero to negative values of \bar{a}_y . For $y \neq 0$, the one-loop term in $\beta_{\bar{a}_y}$, namely $b_{\bar{a}_y}^{(1)}$, is positive-definite and independent of \bar{a}_λ . Hence, provided that the initial values of y and λ at the starting point of the integration are such that one can apply these perturbative calculations, \bar{a}_y decreases toward zero as μ decreases from the UV to the IR. Since for $y \neq 0$, the two-loop term, $b_{\bar{a}_y}^{(2)}$, is negative, it follows that the full two-loop beta function, $\beta_{\bar{a}_y, 2\ell} = \bar{a}_y^2[(1+2r) - 3r\bar{a}_y]$ has a zero, which occurs at

$$\bar{a}_y^* = \frac{1+2r}{3r}, \quad (4.9)$$

independent of \bar{a}_λ . For weaker Yukawa couplings, i.e., $\bar{a}_y < \bar{a}_y^*$, $\beta_{\bar{a}_y, 2\ell} > 0$, so the UV to IR flow is to still weaker Yukawa couplings, while for $\bar{a}_y > \bar{a}_y^*$, $\beta_{\bar{a}_y, 2\ell} < 0$, so that the direction of the UV to IR flow is to larger \bar{a}_y . Note that as r decreases toward 0, \bar{a}_y^* get sufficiently large that one cannot trust the perturbative calculations, so this discussion is restricted to moderate values of r . These results are shown in Fig. 3. For the range of r shown in Fig. 3, $\bar{a}_y^* \sim 1$. As is evident from Eq. (4.9), as $r \rightarrow \infty$, \bar{a}_y approaches the limit $2/3$ from above.

We next discuss the one-loop and two-loop terms in $\beta_{\bar{a}_\lambda}$. The analysis here is more complicated than that for $\beta_{\bar{a}_y}$, because whereas the one-loop and two-loop terms in $\beta_{\bar{a}_y}$ depended only on \bar{a}_y , the one-loop and two-loop terms in $\beta_{\bar{a}_\lambda}$ depend on both \bar{a}_λ and \bar{a}_y . We find that the one-loop term $b_{\bar{a}_\lambda}^{(1)}$ is positive (negative) if \bar{a}_λ is larger (smaller) than the value

$$\bar{a}_\lambda = \frac{1}{2} \left[-r + \sqrt{r(r+2)} \right] \bar{a}_y \quad (4.10)$$

and zero if the equality in Eq. (4.10) holds. The condition in Eq. (4.10) is equivalent to $\bar{a}_y = [1 + \sqrt{1 + (2/r)}] \bar{a}_\lambda$. The solution for \bar{a}_λ in Eq. (4.10) is one of the two solutions of the quadratic equation $b_{\bar{a}_\lambda} = 0$; the solution with the minus sign in front of the square

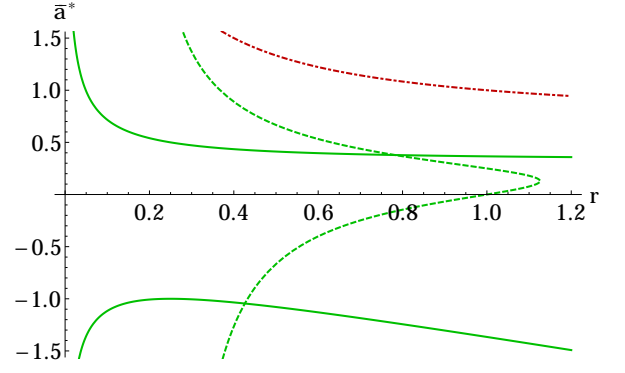


FIG. 3: The fixed point values of (i) \bar{a}_y , denoted as \bar{a}_y^* and shown as the red, dot-dashed curve, and (ii) \bar{a}_λ , denoted as \bar{a}_λ^* and shown as the green solid curve for the case (2,1) and green dashed curve for the (2,2) case, plotted as functions of $r = N_f/N$ (with the LNN limit understood). The curve for \bar{a}_y^* is the same for the (2,1) and (2,2) cases, since, as discussed in the text, $\beta_{\bar{a}_y}$ is independent of \bar{a}_λ to two-loop order. The curves with \bar{a}_λ negative are only formal, since the theory is unstable for $\bar{a}_\lambda \leq 0$, i.e., $\lambda \leq 0$.

root is unphysical because it leads to a negative λ , and similarly in the equivalent solution for \bar{a}_y , the other root with the minus sign in front of the square root is unphysical. The fact that $b_{\bar{a}_\lambda}^{(1)} > 0$ for \bar{a}_λ larger than the value on the right-hand side of Eq. (4.10) means that if the initial value of \bar{a}_λ satisfies this condition, then in the RG flow from the UV to the IR, \bar{a}_λ decreases, and similarly, if the initial value of \bar{a}_λ is smaller than the value on the right-hand side of Eq. (4.10), then \bar{a}_λ increases in the RG flow from the UV to IR.

We come next to the two-loop term in $\beta_{\bar{a}_\lambda}$, namely $b_{\bar{a}_\lambda}^{(2)}$. Because this factorizes into a linear times a quadratic factor in the LNN limit that we consider here, it is somewhat simpler to analyze than $b_{\bar{a}_\lambda}^{(2)}$ for the $SU(2) \otimes U(1)$ model. We find that $b_{\bar{a}_\lambda}^{(2)}$ is negative (positive) if \bar{a}_λ is larger (smaller) than the value

$$\bar{a}_\lambda = \frac{1}{16}(-3 + \sqrt{73}) \bar{a}_y = 0.34650 \bar{a}_\lambda \quad (4.11)$$

(The solution of the quadratic with the opposite sign in front of the square root is unphysical, since it renders λ negative.) The two-loop term $b_{\bar{a}_\lambda}^{(2)}$ vanishes if $\bar{a}_y = 0$ or if the condition in Eq. (4.11) is satisfied. Thus, for large \bar{a}_λ relative to \bar{a}_y , as least to the extent that our perturbative calculations still apply, we thus find that the one-loop and two-loop terms in the $\beta_{\bar{a}_\lambda, 2\ell}$ have the opposite signs; $b_{\bar{a}_\lambda}^{(1)} > 0$, while $b_{\bar{a}_\lambda}^{(2)} < 0$. Similarly, for sufficiently small \bar{a}_λ relative to \bar{a}_y , these terms again have opposite signs; $b_{\bar{a}_\lambda}^{(1)} < 0$, while $b_{\bar{a}_\lambda}^{(2)} > 0$. It is thus plausible that the full two-loop $\beta_{\bar{a}_\lambda, 2\ell}$ would have a zero, where these terms cancel each other.

In Fig. 3 we show our solutions for the value of the fixed point in the variable \bar{a}_λ as a function of r . (Here and elsewhere, it is implicitly understood that the LNN limit

has been taken.) The value of r determines the value of the fixed point in \bar{a}_y , the existence or non-existence of a fixed point in \bar{a}_λ , and, in the former case, its value. The solutions that yield a fixed point \bar{a}_λ^* at negative values are only formal, since the theory is unstable for $\bar{a}_\lambda < 0$, i.e., $\lambda < 0$. If \bar{a}_λ is negative but $|\bar{a}_\lambda|$ is sufficiently small, the theory may be metastable, but considerations of metastability and estimates of tunneling times are beyond the scope of our present analysis. Thus, as regards \bar{a}_λ , there is only a single physical fixed point, \bar{a}_λ^* , and the calculation for the (2,1) case yields a value of $\bar{a}_\lambda^* \simeq 0.5$ in the range of r shown, for which perturbation theory may be reliable down to $r \simeq 0.2$. As $r \rightarrow \infty$, this curve for \bar{a}_λ^* approaches the limit $1/3$. For the (2,2) case, if $r < 1.0$, there is also only one physical (positive) fixed point, \bar{a}_λ^* , but its value grows more rapidly as r decreases, so that one anticipates significant corrections to the two-loop perturbative result already for r decreasing below $r \simeq 0.4$. In the narrow interval of r between $r = 1.0$ and the value

$$r_{\text{merger}}^{(2,2)} = \frac{31 + 12\sqrt{3}}{46} = 1.12575 \quad (4.12)$$

there are two physical fixed points for \bar{a}_λ . We shall refer to these as the upper and lower fixed points. As r increases through the value $r_{\text{merger}}^{(2,2)}$, the upper and lower fixed points in \bar{a}_λ merge and disappear. This happens when the solution to the equation $\beta_{\bar{a}_y, 2\ell} = \beta_{\bar{a}_\lambda, 2\ell} = 0$ becomes complex, which happens at $r = r_{\text{merger}}^{(2,2)}$.

C. RG Flows

Here we present the results of our integration of the beta functions calculated to various loop orders. Our convention is to start the analysis at a high value of μ in the UV, integrate the renormalization-group equations for \bar{a}_y and \bar{a}_λ , and follow the flow from the UV to the IR, and this is indicated by the direction of the arrows. In Fig. 4 we plot the RG flows for $r = 0.5$ and

$$\bar{a}_y < \frac{1}{4\pi}, \quad \bar{a}_\lambda < \frac{1}{4\pi}, \quad \text{i.e.,} \quad \frac{y^2 N}{4\pi} < 1, \quad \frac{\lambda N}{4\pi} < 1. \quad (4.13)$$

We find that for this value of r and range of \bar{a}_y and \bar{a}_λ , the theory has only the IR fixed point at the IR-free point

$$(\bar{a}_y^*, \bar{a}_\lambda^*) = (0, 0). \quad (4.14)$$

This can be understood as a result of the fact that the one-loop expression for β_{a_y} , namely, $\beta_{a_y, 1\ell}$, is positive and independent of a_λ , so as μ decreases from the UV to the IR, \bar{a}_y always decreases. Although the one-loop result for $\beta_{\bar{a}_\lambda}$, namely $\beta_{\bar{a}_\lambda, 1\ell}$, could initially be negative if the initial value of \bar{a}_y is such that $\bar{a}_y > (1 + \sqrt{13})\bar{a}_\lambda$, as discussed above, $\beta_{\bar{a}_\lambda, 1\ell}$ will eventually pass through zero and become positive as \bar{a}_y decreases through this zero, and as the flow continues toward the IR thereafter, $\beta_{\bar{a}_\lambda, 1\ell}$ will remain positive. This causes \bar{a}_λ to vanish in the IR.

These results also provide an answer to a question that we posed at the beginning, namely how robust the perturbative calculation of the RG flows are to the inclusion of higher-loop terms in the beta function. For this range (4.13) of \bar{a}_y and \bar{a}_λ , all four cases (1,1), (1,2), (2,1), and (2,2) yield qualitatively similar flows. This serves as a strong indication that for this range (4.13), our perturbative calculations are reliable.

Next, we increase r from 0.5 to 1.1. The results are shown in Fig. 5. We reach the same qualitative conclusions for this case $r = 1.1$ as for $r = 0.5$.

We next study a larger range of \bar{a}_y and \bar{a}_λ , namely $0 < \bar{a}_y < 1.5$ and $0 < \bar{a}_\lambda \leq 1.5$. We show the RG flows for $r = 0.5$ and $r = 1.1$ in Figs. 6 and 7.

For reference, in these plots we distinguish three regions: (i) a white square region where $0 \leq \bar{a}_y \leq 1/(4\pi)$ and $0 \leq \bar{a}_\lambda \leq 1/(4\pi)$; (ii) a light gray region where $1/(4\pi) \leq \bar{a}_y \leq 1$ and $1/(4\pi) \leq \bar{a}_\lambda \leq 1$ ($1/(4\pi) \leq \bar{a}_y \leq 0.75$ and $1/(4\pi) \leq \bar{a}_\lambda \leq 0.75$ in Fig. 7); and (iii) a dark gray region where $1 \leq \bar{a}_y \leq 1.5$ and $1 \leq \bar{a}_\lambda \leq 1.5$ ($0.75 \leq \bar{a}_y \leq 1.5$ and $0.75 \leq \bar{a}_\lambda \leq 1.5$ in Fig. 7). In the case where $r = 0.5$ (Figure 6), the four light gray regions are still quite similar, but now the inclusion of the two-loop term in $\beta_{\bar{a}_\lambda}$ has a significant effect. In the left-hand plots where this term is not included, we note that the flows that reach the fixed points seem to be attracted to a central flow, which, in the (2,1) (lower left) plot is identified with the one flowing in the eigendirection from the upper fixed point. In the right-hand plots that include the two-loop term in $\beta_{\bar{a}_\lambda}$, this behavior is reversed for relatively large values of \bar{a}_y . In (1,1) and (2,1) cases, the RG flows in the light gray region where $\bar{a}_y \leq 1$ and $\bar{a}_\lambda \leq 1$, look similar to the flows in the white square region where $\bar{a}_y \leq 1/(4\pi)$ and $\bar{a}_\lambda \leq 1/(4\pi)$.

The largest changes in the flows occur in the dark gray area where \bar{a}_y and \bar{a}_λ are largest. When considering this region, it is important to recall that this is where we expect perturbation theory to break down, partly because higher-order terms in the beta functions are of comparable size compared with lower-order terms, and partly because completely nonperturbative effects such as fermion condensates can appear for such strong values of the couplings. However, continuing in the context of the perturbative analysis, we see that fixed points appear in the (2,1) and (2,2) plots, and correspondingly the flows are changed by their presence.

The inclusion of the two-loop term in $\beta_{\bar{a}_\lambda}$ fundamentally changes the nature of the fixed points. In the (2,1) plot, we see that the non-trivial fixed point is attractive along the vertical direction, and repulsive along the approximately horizontal direction, but the fixed point in the (2,2) case occurs at a roughly similar position, it is now repulsive in all directions.

In Fig. 7, we note that (1,1), (1,2), and (2,1) plots are similar to those in Fig. 6, except that the fixed point in the (2,1) plot now occurs at a value of $\bar{a}_y < 1$. However, in the (2,2) plot, the flows are very different. Most dramatically, the lower fixed point (see Fig. 3) has become

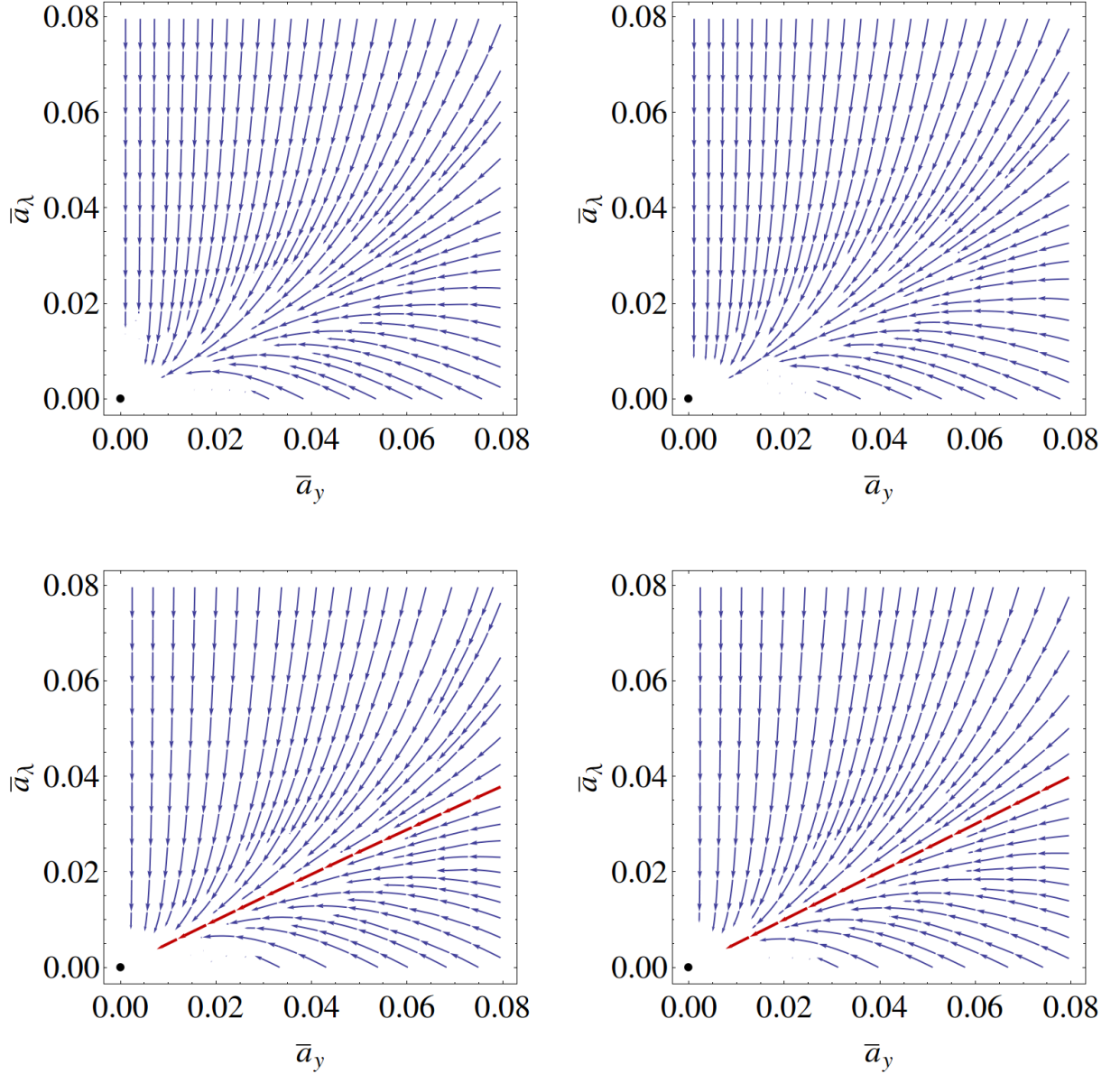


FIG. 4: The renormalization-group flows for $r = 0.5$ with $0 \leq \bar{a}_y \leq 1/(4\pi)$ and $0 \leq \bar{a}_\lambda \leq 1/(4\pi)$. The figures correspond to the following choices of inclusion of different-loop terms in the beta functions: upper left: (1,1); upper right: (1,2); lower left: (2,1); lower right: (2,2). The red flows in the (2,1) and (2,2) cases originate along the eigendirection of the upper fixed point (see Figure 3).

positive, and is very close to merging with the upper one.

Thus, our comparative calculations of RG flows for these (1,1), (1,2), (2,1), and (2,2) cases in this model show that a perturbative calculation of the RG flows and fixed points is reasonably reliable for the region $0 \leq \bar{a}_y \lesssim 1/(4\pi)$ and $0 < \bar{a}_\lambda \lesssim 1/(4\pi)$ but is unreliable when these variables increase to sizes of order 1 or greater.

V. CONCLUSIONS

In summary, in this paper we have calculated renormalization-group flows and resultant fixed points in scalar-fermion theories depending on two couplings, a Yukawa coupling y and a quartic scalar self-coupling λ . We have addressed a fundamental question pertaining to the RG flows in these theories, namely the question of the range of values of y and λ for which these flows can be determined reliably using the beta functions β_y and β_λ calculated up to various respective loop orders. To inves-

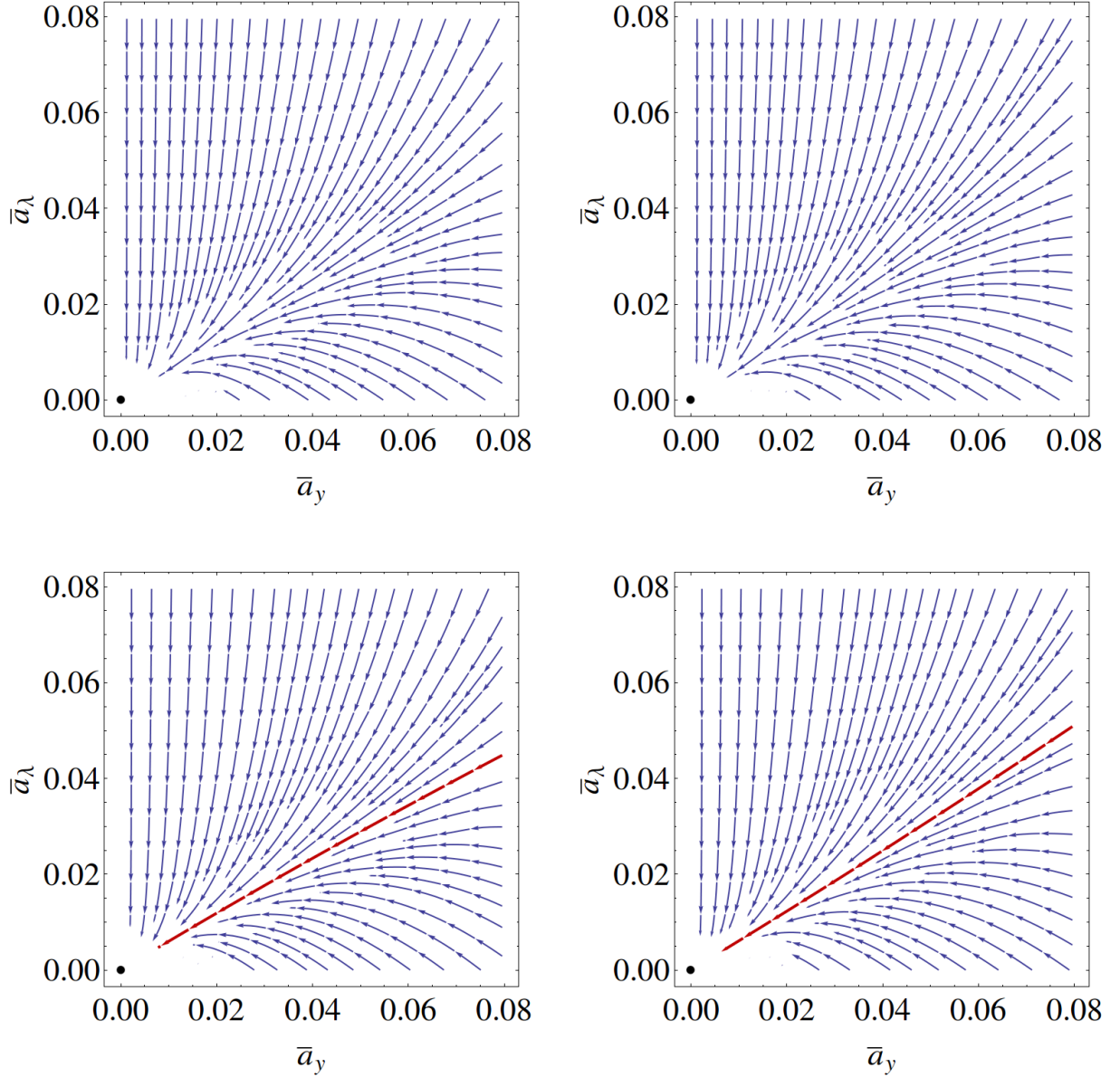


FIG. 5: The renormalization-group flows for $r = 1.1$ with $0 \leq \bar{a}_y \leq 1/(4\pi)$ and $0 \leq \bar{a}_\lambda \leq 1/(4\pi)$. The figures correspond to the following choice of inclusion of different loop-order terms in the beta functions: upper left: (1,1); upper right: (1,2); lower left: (2,1); lower right: (2,2). The red flows in the (2,1) and (2,2) cases originate along the eigendirection of the upper fixed point (see Figure 3).

tigate this, we have focused on two models and have calculated these flows using the n -loop beta function $\beta_{y,n\ell}$ and the k -loop beta function $\beta_{\lambda,k\ell}$ with $(n,k) = (1,1)$, $(1,2)$, $(2,1)$, $(2,2)$. We have presented our results in a set of convenient variables, a_y and a_λ for a model with a global $SU(2) \otimes U(1)$ symmetry group and \bar{a}_y and \bar{a}_λ in the limit (4.4) of a model with a $SU(N) \otimes SU(N_f) \otimes U(1)$ global symmetry group. Our results provide a quantitative answer to this question. In future work, it would be worthwhile to extend the perturbative calculations of the beta functions to higher loop orders and to investigate connections between semiperturbative properties

at moderately strong coupling and nonperturbative phenomena in the scalar and fermion sectors of the models.

Acknowledgments

This research was partly supported by the Centre for Particle Physics Phenomenology-Origins (CP3-Origins) of the Southern Denmark University which is partially funded by the Danish National Research Foundation, grant number DNRF90 (E.M.) and by the NSF grant

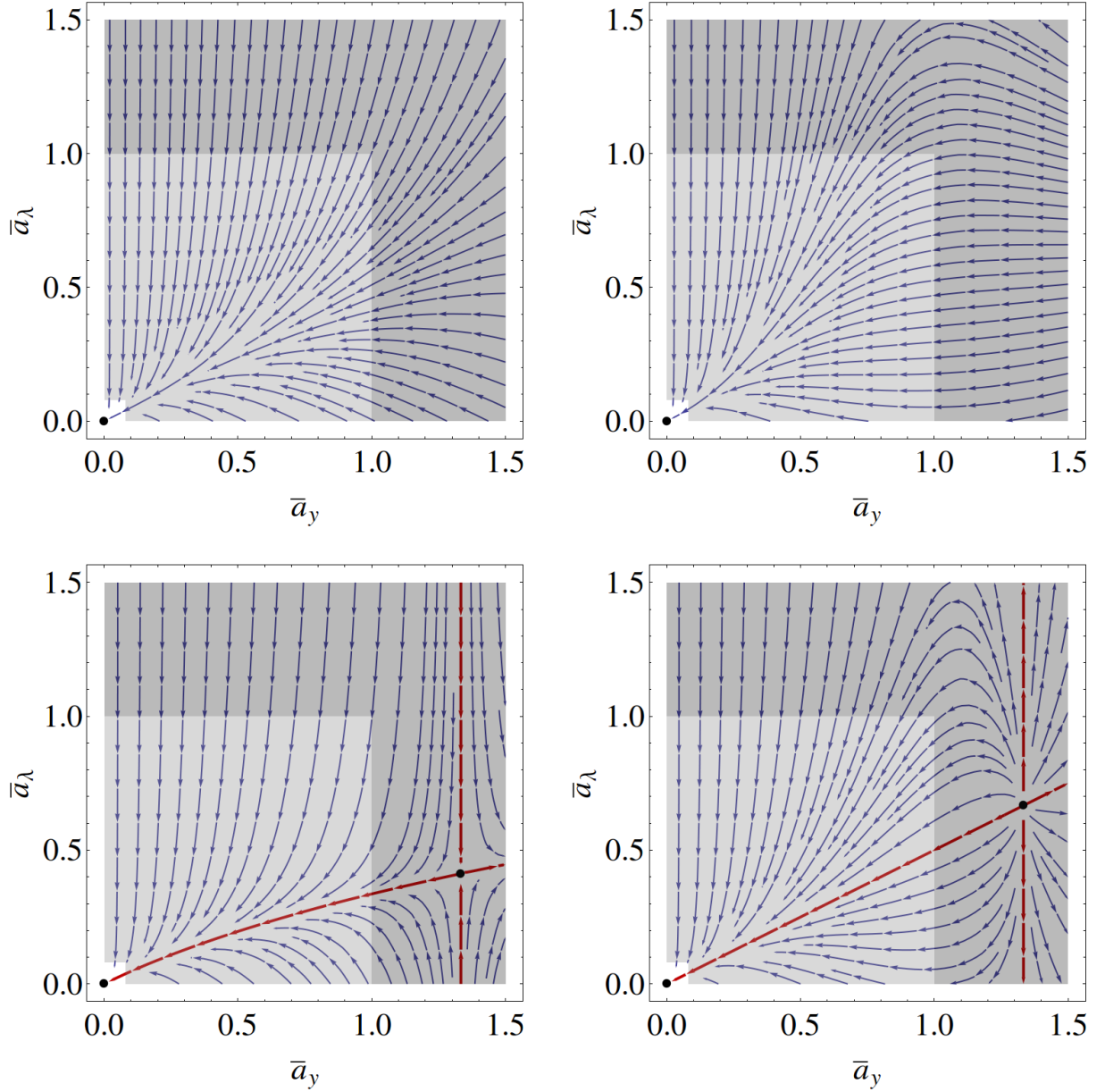


FIG. 6: The renormalization-group flows for $r = 0.5$ with $0 \leq \bar{a}_y \leq 1.5$ and $0 \leq \bar{a}_\lambda \leq 1.5$. The white square region is where $0 \leq \bar{a}_y \leq 1/(4\pi)$ and $0 \leq \bar{a}_\lambda \leq 1/(4\pi)$; the light gray region is where $1/(4\pi) \leq \bar{a}_y \leq 1$ and $1/(4\pi) \leq \bar{a}_\lambda \leq 1$; and the dark gray region occupies the rest of the plot. The figures correspond to the following choices of inclusion of different loop-order terms in the beta functions: (1,1) (upper left); (1,2) (upper right); (2,1) (lower left); and (2,2) (lower right). The red flows in (2,1) and (2,2) originate along the eigendirections of the fixed points.

NSF-PHY-13-16617 (R.S.).

[1] Some early studies on the renormalization group in quantum field theory include E. C. G. Stueckelberg and A. Peterman, *Helv. Phys. Acta* **26**, 499 (1953); M. Gell-Mann and F. Low, *Phys. Rev.* **95**, 1300 (1954); N. N. Bogolubov and D. V. Shirkov, *Doklad. Akad. Nauk SSSR* **103**, 391 (1955); C. G. Callan, *Phys. Rev. D* **2**, 1541 (1970); K. Symanzik, *Commun. Math. Phys.* **18**, 227 (1970). See

also K. Wilson, *Phys. Rev. D* **3**, 1818 (1971).
 [2] W. E. Caswell, *Phys. Rev. Lett.* **33**, 244 (1974); D. R. T. Jones, *Nucl. Phys. B* **75**, 531 (1974).
 [3] T. Banks and A. Zaks, *Nucl. Phys. B* **196**, 189 (1982).
 [4] E. Gardi and M. Karliner, *Nucl. Phys. B* **529**, 383 (1998); E. Gardi, G. Grunberg and M. Karliner, *JHEP* **9807**, 007 (1998); T. A. Ryttov and R. Shrock, *Phys. Rev. D* **83**,

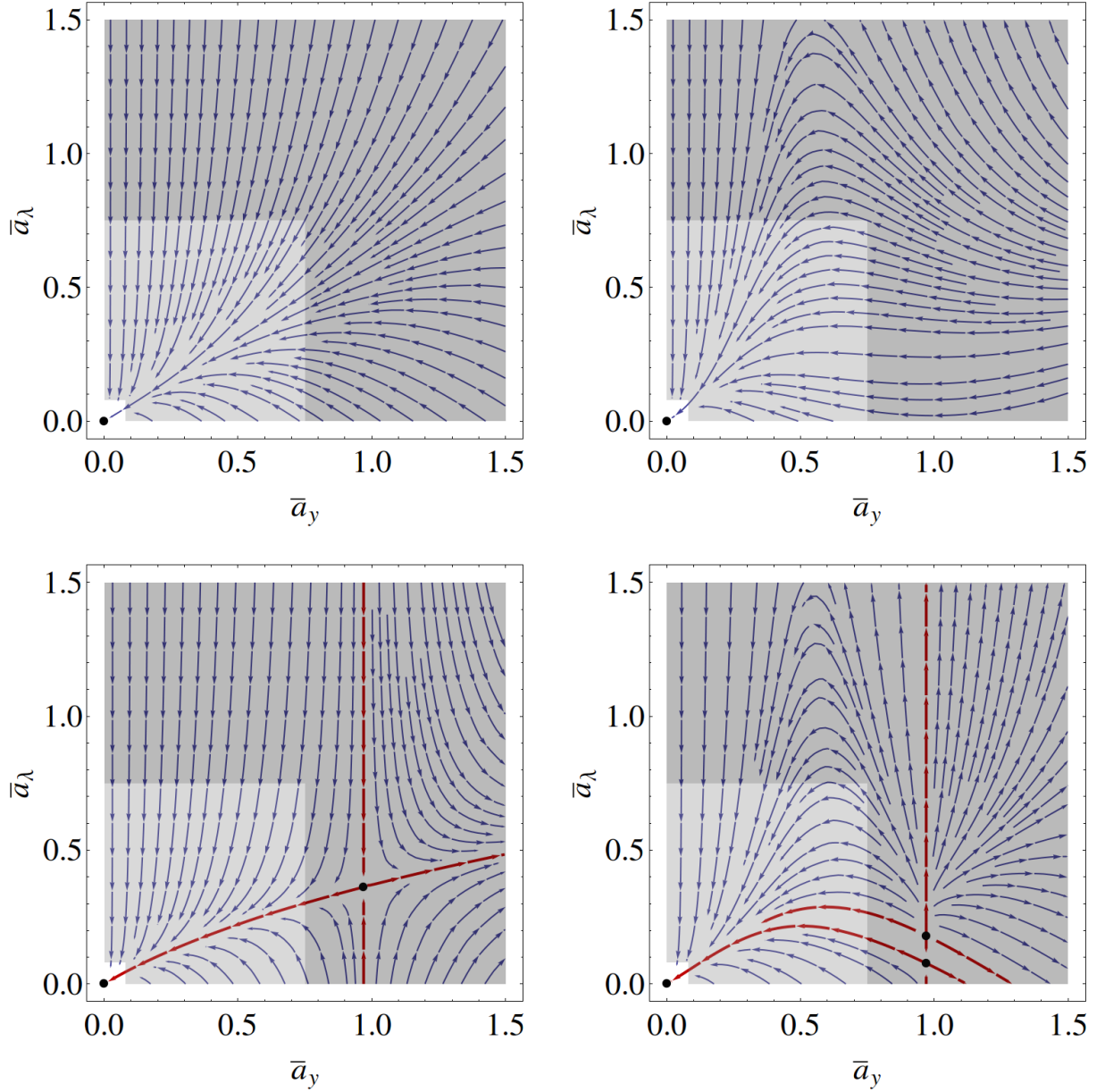


FIG. 7: The renormalization-group flows for $r = 1.1$ with $0 \leq \bar{a}_y \leq 1.5$ and $0 \leq \bar{a}_\lambda \leq 1.5$. The white square region is where $0 \leq \bar{a}_y \leq 1/(4\pi)$ and $0 \leq \bar{a}_\lambda \leq 1/(4\pi)$; the light gray region is where $1/(4\pi) \leq \bar{a}_y \leq 0.75$ and $1/(4\pi) \leq \bar{a}_\lambda \leq 0.75$; and the dark gray occupies the rest of the plot. The figures correspond to the following choices of inclusion of different loop-order terms in the beta functions: (1,1) (upper left); (1,2) (upper right); (2,1) (lower left); and (2,2) (lower right). The red flows in (2,1) and (2,2) originate along the eigendirections of the fixed points.

- 056011 (2011) [arXiv:1011.4542]; C. Pica and F. Sannino, Phys. Rev. D **83**, 035013 (2011) [arXiv:1011.5917]; T. A. Ryttov and R. Shrock, Phys. Rev. D **85**, 076009 (2012) [arXiv:1202.1297]; R. Shrock, Phys. Rev. D **87**, 105005 (2013) [arXiv:1301.3209]; R. Shrock, Phys. Rev. D **87**, 116007 (2013) [arXiv:1302.5434].
- [5] B. Holdom, Phys. Lett. B **694**, 74 (2010).
- [6] R. Shrock, Phys. Rev. D **88**, 036003 (2013) [arXiv:1305.6524]; R. Shrock, Phys. Rev. D **89**, 045019 (2014) [arXiv:1311.5268].
- [7] Some of the many recent papers on this include J. Ellis, J. R. Espinosa, G. F. Giudice, A. Hoecker, and A. Riotto,

Phys. Lett. B **679**, 369 (2009); M. Shaposhnikov and C. Wetterich, Phys. Lett. B **683**, 196 (2010); F. Bezrukov and M. Shaposhnikov, JHEP **0907**, 089 (2009); J. Elias-Miro, J. R. Espinosa, G. F. Giudice, G. Isadori, A. Riotto, and A. Strumia, Phys. Lett. B **709**, 222 (2012) [arXiv:1112.3022]; G. Degrandi, S. Di Vita, J. Elias-Miro, J. R. Espinosa, G. F. Giudice, G. Isadori, and A. Strumia, JHEP **1208**, 098 (2012) [arXiv:1205.6497]; F. Bezrukov, M. Yu. Kalmykov, B. A. Kniehl, and M. Shaposhnikov, JHEP **1210**, 140 (2012) [arXiv:1205.2893]; L. A. Anchordoqui, I. Antoniadis, H. Goldberg, X. Huang, D. Lust, T. Taylor, and B. Vlcck, JHEP **1302**,

- 074 (2013) [arXiv:1208.2821]; I. Masina, Phys. Rev. D **87**, 5 (2013) 053001 [arXiv:1209.0393]; F. Jegerlehner, arXiv:1305.6652; D. Buttazzo, G. Degrandi, G. F. Giudice, F. Sala, A. Salvio, and A. Strumia, JHEP **1312**, 089 (2013) [arXiv:1307.3536]; V. Branchina, E. Messina, Phys. Rev. Lett. **111**, 241801 (2013) [arXiv:1307.5193]; H. Gies, C. Gneiting, and R. Sondenheimer, Phys. Rev. D **89**, 045012 (2014) [arXiv:1308.5075]; E. Eichten, talk at CP3 Workshop, Southern Denmark Univ. (Aug. 2013); C. Hill, arXiv:1401.4185.
- [8] M. Holthausen, K. S. Lim, and M. Lindner, JHEP **1202**, 037 (2012) [arXiv:1112.2415]; K. G. Chetyrkin and M. F. Zoller, JHEP **1206**, 033 (2012) [arXiv:1205.2892]; K. G. Chetyrkin and M. F. Zoller, JHEP **1304**, 091 (2013); Erratum-ibid. 1309, 155 (2013) 155, [arXiv:1303.2890]; L. N. Mihaila, J. Salomon, and M. Steinhauser, arXiv:1208.3357.
- [9] O. Antipin, M. Gillioz, J. Krog, E. Mølgaard, and F. Sannino, JHEP **1308**, 034 (2013), [arXiv:1306.3234]; O. Antipin, M. Mojaza, and F. Sannino, arXiv:1310.0957 and references therein.
- [10] H. Yukawa, Proc. Phys. Math. Soc. Jap. **17**, 48 (1935).
- [11] T. P. Cheng, E. Eichten, and L.-F. Li, Phys. Rev. D **9**, 2259 (1974).
- [12] L. Maiani, G. Parisi and R. Petronzio, Nucl. Phys. B **136**, 115 (1978); R. Flores and M. Sher, Phys. Rev. D **27**, 1679 (1983); M. A. Beg, C. Panagiotakopoulos and A. Sirlin, Phys. Rev. Lett. **52**, 883 (1984); M. Lindner, Z. Phys. C **31**, 298 (1986).
- [13] I-H. Lee and R. E. Shrock, Phys. Rev. Lett. **59**, 14 (1987); I-H. Lee and R. E. Shrock, Phys. Lett. B **199**, 541 (1987); J. Shigemitsu, Phys. Lett. B **189**, 164 (1987); I-H. Lee and R. E. Shrock, Nucl. Phys. B **305**, 305 (1988); J. Shigemitsu, Phys. Lett. B **226**, 364 (1989); A. Hasenfratz and T. Neuhaus, Phys. Lett. B **220**, 435 (1989); I-H. Lee, J. Shigemitsu, and R. E. Shrock, Nucl. Phys. B **330**, 225 (1990); I-H. Lee, J. Shigemitsu, and R. E. Shrock, Nucl. Phys. B **334**, 265 (1990); A. Hasenfratz, W.-Q. Liu, and T. Neuhaus, Phys. Lett. B **236**, 339 (1990); L. Lin, I. Montvay, H. Wittig, and G. Münster, Nucl. Phys. B **355**, 511 (1991); J. Shigemitsu, Nucl. Phys. Proc. Suppl. **20**, 515 (1991); R. E. Shrock, in *Quantum Fields on the Computer*, ed. M. Creutz (World Scientific, Singapore, 1992), pp. 150-210.
- [14] Z. Fodor, K. Holland, J. Kuti, D. Negradi, and C. Schroeder, Proc. Sci. LAT2007 (2007) 056 [arXiv:0710.3151]; P. Gerhold and K. Jansen, JHEP **0907**, 094 (2010) [arXiv:0902.4135]; P. Gerhold and K. Jansen, JHEP **1004**, 094 (2010) 094 [arXiv:1002.4336].
- [15] B. Grinstein and P. Uttayarat, JHEP **1107**, 038 (2011) [arXiv:1105.2370]; O. Antipin, S. Di Chiara, M. Mojaza, E. Mølgaard, and F. Sannino, Phys. Rev. D **86**, 085009 (2012) [arXiv:1205.6157]. O. Antipin, M. Mojaza and F. Sannino, Phys. Lett. B **712**, 119 (2012) [arXiv:1107.2932].
- [16] O. Antipin, M. Mojaza, and F. Sannino, Phys. Rev. D **87**, 096005 (2013) [arXiv:1208.0987]; O. Antipin, M. Gillioz, E. Mølgaard, and F. Sannino, Phys. Rev. D **87**, 125017 (2013) [arXiv:1303.1525].
- [17] B. Grinstein, A. Stergiou, and D. Stone, JHEP **1311**, 195 (2013) [arXiv:1308.1096].
- [18] G. 't Hooft, Nucl. Phys. B **61**, 455 (1973); W. A. Bardeen, A. J. Buras, D. W. Duke, and T. Muta, Phys. Rev. D **18**, 3998 (1978).
- [19] T. A. Ryttov and R. Shrock, Phys. Rev. D **86**, 065032 (2012) [arXiv:1206.2366]; Phys. Rev. D **86**, 085005 (2012) [arXiv:1206.6895].
- [20] T. A. Ryttov, Phys. Rev. D **89**, 016013 (2014) [arXiv:1309.3867].
- [21] There have been many studies of nonrelativistic bound states due to Yukawa interactions, but these are not directly relevant to our work, since our models are constructed to be invariant under global chiral symmetries and hence to avoid any bare fermion terms, so that the fermions are ultrarelativistic. Some explorations of possible relativistic fermion-fermion bound states resulting from a strong Yukawa interaction include St. Glazek, A. Harindranath, S. Pinsky, J. Shigemitsu, and K. Wilson, Phys. Rev. D **47**, 1599 (1993); M. Mangin-Brinet, J. Carbonell, and V. A. Karmanov, Phys. Rev. D **64**, 125005.
- [22] S. R. Coleman and E. J. Weinberg, Phys. Rev. D **7**, 1888 (1973). E. Gildener and S. Weinberg, Phys. Rev. D **13**, 3333 (1976).
- [23] P. Q. Hung, Phys. Rev. Lett. **42**, 873 (1979); A. D. Linde, Phys. Lett. B **92**, 119 (1980); H. D. Politzer and S. Wolfram, Phys. Lett. B **82**, 242 (1979); M. Sher, Phys. Rep. **179**, 273 (1989).
- [24] The purpose of this assumption of negligibly small m_ϕ compared with the range of μ of interest for our RG flows is to ensure that the ϕ field is dynamical; if m_ϕ were $\gg \mu$ for the values of μ of interest, then we could integrate it out, obtaining a low-energy effective field theory consisting of just the fermions ψ and χ with a resultant four-fermion operator $\propto (1/m_\phi^2) \sum_a [\bar{\psi}_{a,L} \chi_R] [\bar{\chi}_R \psi_L^a] + h.c.$.
- [25] M. Fischler and J. Oliensis, Phys. Lett. B **119**, 385 (1982); Phys. Rev. D **28**, 2027 (1983); M. E. Machacek and M. T. Vaughn, Nucl. Phys. B **236**, 221 (1984); M. E. Machacek and M. T. Vaughn, Nucl. Phys. B **249**, 70 (1985); I. Jack and H. Osborn, Nucl. Phys. B **249**, 472 (1985); C. Ford, I. Jack, and D. R. T. Jones, Nucl. Phys. B **387**, 373 (1992); erratum ibid. B **504**, 551 (1997); V. Barger, M. S. Berger, and P. Ohmann, Phys. Rev. D **47**, 1093 (1993); M.-x. Luo, H.-w. Wang and Y. Xiao, Phys. Rev. D **67**, 065019 (2003);